ALTITUDE SPECIFICATION OF CLOUD MOTION WINDS

W.L. Smith and Richard Frey

Cooperative Institute for Meteorological Satellite Studies
University of Wisconsin-Madison
Madison, Wisconsin

ABSTRACT

Aircraft high spectral resolution interferometer measurements of upwelling radiance are used to simulate various spectral radiance observations made from geostationary satellite sensors. Using the simulated satellite observations, various cloud height retrieval methods are tested and the results compared to accurate airborne LIDAR measurements coincident with the infrared observations. In this study methods currently used for estimating cloud height from Japanese, United States, and European satellites were intercompared. The most accurate results were those obtained using a combination of 13.3 μm CO_2 and 11.1 μm "Window" channel radiances. It is also demonstrated that the use of 6.7 μm H_2O channel radiances produce a significant improvement over results achieved with 11.1 μm window radiances alone; however, the water vapor channel results are still inferior to the CO_2 channel estimates. Thus, attempts should be made to include a 13.3 μm CO_2 channel on future geostationary satellite imaging radiometers used to produce cloud tracked winds for meteorological applications.

1. Introduction

The international geostationary satellite system used for cloud motion wind determination is comprised of sensors with varying spectral infrared radiance measurement capabilities. The capabilities range from a single 11 μm "window" channel (the current GMS and INSAT) to channels operating in the 11 μm "window" and the 6.7 μm water vapor absorption region (the METEOSAT) to twelve infrared spectral channels which measure surface, cloud, water vapor, and carbon dioxide emission between 3.9 and 15 μm (the GOES-VAS). These various infrared spectral radiance measurement capabilities impact the accuracy to which cloud heights can be determined. The accuracy and utility of wind vectors specified from cloud motions are limited by the spectral infrared measurement capabilities of each sensor.

There are three basic techniques used for cloud height assignment, depending upon the sensor capability:

(1) "Brightness Temperature Comparison"
(2) Absorption Channel "Slicing"
(3) "Linear Extrapolation" of window vs. absorption channel radiance.

In this paper the three methods noted above are discussed. Results are presented from their application to a "Cirrus" cloud situation. The data set used consists of High resolution Infrared Spectrometer (HIS) radiance observations from the high altitude (20 km) NASA ER-2 aircraft (Revercomb, et. al., 1988) from which infrared observations corresponding to any of the geostationary satellite instruments can be simulated by spectral convolution of the data (Smith and Frey, 1990). Also aboard the ER-2 was a "LIDAR" instrument which provided simultaneous measurements of cloud top altitude with an accuracy of 100 meters (Spinhirne, 1982). A near time coincident special radiosonde observation was used in the radiative transfer calculations needed for testing the various cloud height assignment methods.

The particular data set presented here pertains to November 2, 1986, the last day of the "First ISCCP Regional Experiment (FIRE)" conducted over Wisconsin. Figure 1 shows an example "HIS" spectrum with the spectral bandwidths assumed for simulating the geostationary satellite instrument channels shown as bars.

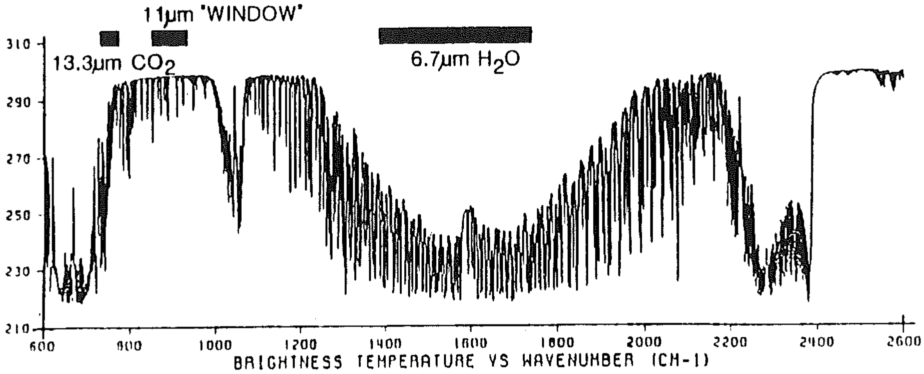

Figure 1: Spectrum of upwelling radiance (in equivalent Brightness Temperature units) with "bars" denoting the geostationary satellite spectral channels considered here.

2. Methods

(a.) Brightness Temperature Comparison

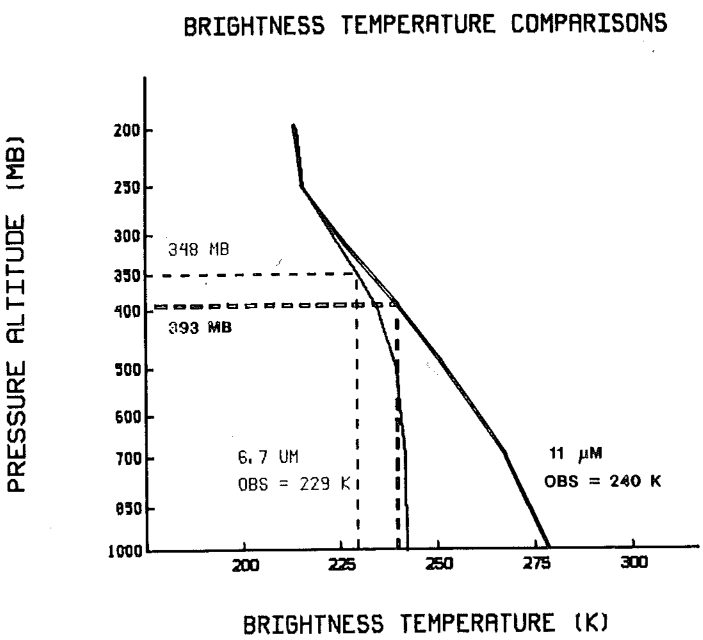

The so-called "Brightness Temperature Comparison" method consists of comparing the brightness temperature observed for a particular spectral channel with a cloud pressure profile of brightness temperature. The brightness temperature profile is generated by radiative transfer calculation using a temperature and water vapor profile and assuming "opaque" cloud conditions for each pressure level. Figure 2 graphically illustrates the technique.

If one uses spectral channels where there is little atmospheric contribution above the cloud level (e.g., an 11 μm "window" channel), the accuracy of the technique is primarily limited by the opacity of the cloud and secondarily by the accuracy of the

Figure 2: Illustration of "Brightness Temperature Comparison" method. The curves denote the brightness temperature which should be observed as a function of the pressure altitude of an opaque cloud.

temperature profile. If an absorption channel (e.g., 6.7 μm water vapor) is used, then the accuracy is also compromised by the accuracy of the prespecified absorbing gas (e.g., water vapor) profile above the cloud level. The dependency of the cloud height accuracy on the specification accuracy of the absorbing gas above the cloud decreases with increasing cloud height.

(b.) CO_2 and H_2O "Slicing"

The so-called slicing method (Menzel, Smith, and Stewart, 1983) is based upon the assumption that the "effective cloud amount" (defined as the product of the fractional cloud cover and the cloud emissivity) is the same for two spectral channels with significantly different molecular absorption characteristics. In this case it can be shown (Smith and Platt, 1978) that

$$\frac{\delta R(\upsilon_1)}{\delta R(\upsilon_2)} = \frac{\varepsilon(\upsilon_1)\delta N}{\varepsilon(\upsilon_2)\delta N} \frac{\int_{p_c}^{p_s} \tau(\upsilon_1,p)dB(\upsilon_1,p)}{\int_{p_c}^{p_s} \tau(\upsilon_2,p)dB(\upsilon_2,p)} = f(p_c) \qquad (1)$$

where $f(p_c)$ is the cloud pressure function, δR is the deviation of the cloudy radiance observation from either a "clear column" radiance or a radiance observation for a smaller fraction of the same cloud at the same altitude, $\varepsilon(\upsilon)$ is the cloud emissivity, δN is the difference in the fractional cloud coverage for the two observations forming δR, τ is the transmission of the atmosphere between the sensor and the pressure level p, and B is "Planck" radiance which is a unique function of temperature for a particular wavenumber υ. For satellite spectral channels which have a finite spectral bandwidth, all quantities in equation (1) are integrated over wavenumber with a spectral weighting provided by the instruments response function.

Since it assumed that both spectral observations (υ_1 and υ_2) are obtained for the same field of view at the same time, δN cancels in (1). If one can assume $\varepsilon(\upsilon_1) = \varepsilon(\upsilon_2)$, then it can be seen that the observed ratio, $\delta R(\upsilon_1)/\delta R(\upsilon_2)$, is uniquely related to the cloud pressure, p_c, given a profile of the temperature and absorbing gas concentration. Figure 3 shows a plot of the absorption coefficient as a function of wavelength (the inverse of "wavenumber") for ice and water. It can be seen that for cirrus (i.e., ice) cloud, the emissivity in the 11-12 μm "window" region is approximately the same at that in the 13-14 μm CO_2 absorption region. Thus, the use of 11 μm and 13.3 μm channels is generally used in the application of the "slicing" assignment method for cirrus cloud altitude. It is noteworthy that the ice absorption (i.e., emissivity) in the 6.7 μm water vapor absorption region is less than that at 11 μm. It can be seen from equation (1) that if $\varepsilon(\upsilon_1) < \varepsilon(\upsilon_2)$, then $\delta R(\upsilon_1)/\delta R(\upsilon_2)$ will lead to an underestimate of $f(p_c)$ which in turn leads to and overestimate of the cloud pressure (i.e., an erroneously low cloud altitude estimate). Figure 4 shows a graphical illustration of the technique applied to a single case for November 2, 1986. In the application of the technique, the 11 μm window channel (figure 1) is always used for the denominator of (1). The difference in the slopes of the cloud pressure functions for water vapor and carbon dioxide is due mainly to the order of magnitude of "Planck" radiance variation between 6.7 μm and 13.3 μm for a given blackbody temperature rather than due to the difference in the atmospheric transmission function for the two spectral regions. It is noted that water vapor slicing leads to a higher pressure altitude (lower geometric altitude) estimate than does CO_2 slicing and this is due to the lower ice cloud emissivity (i.e., absorption) at 6.7 μm than at 13.3 μm, as shown in figure 3.

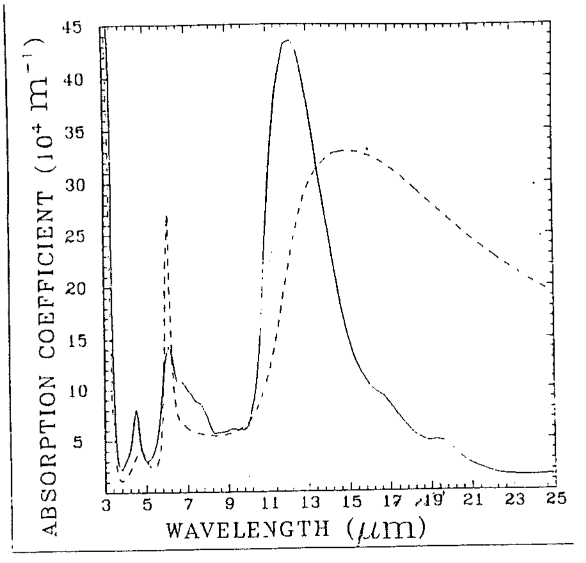

Figure 3: Absorption coefficient for ice (solid curve) and water (dashed) calculated using the imaginary parts of the index of refraction for ice and water as tabulated by Warren (Warren, S.G., 1984: Optical constants of ice from the ultraviolet to the microwave. Appl. Opt., 23, 1206-1225).

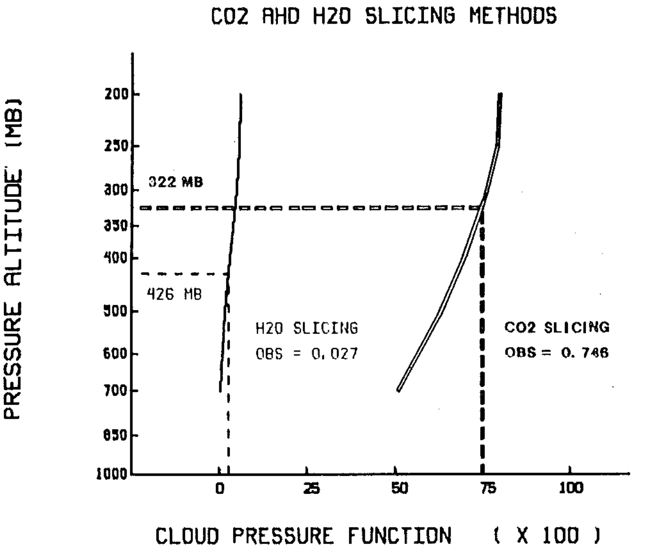

Figure 4: Illustration of the "Slicing" method of cloud height retrieval. The curves denote a cloud function which depends solely on cloud pressure (i.e., not cloud amount or emissivity).

3. "Linear Extrapolation"

The "linear extrapolation" method (Szejwach, 1982; Schmetz, 1989) is similar to the "slicing" method except that one does not impose the assumption that the cloud emissivity for the two spectral channels is the same. Equation (1) can be rewritten as

$$R(\upsilon_1) = \left[R_0(\upsilon_1) - \frac{\varepsilon(\upsilon_1)}{\varepsilon(\upsilon_2)} f(p_c) R_0(\upsilon_2) \right] + \frac{\varepsilon(\upsilon_1)}{\varepsilon(\upsilon_2)} f(p_c)\, R(\upsilon_2) \qquad (2)$$

$$\text{where } f(p_c) = \int_{p_c}^{p_s} \tau(\upsilon_1, p) \frac{\delta B(\upsilon_1, p)}{dp}\, dp \Big/ \int_{p_c}^{p_s} \tau(\upsilon_2, p) \frac{\delta B(\upsilon_2, p)}{dp}\, dp$$

and R_0 corresponds to a "clear column" or more cloud free measurement condition. Thus, for a constant cloud pressure, p_c, and a constant cloud type (i.e., $\varepsilon(\upsilon_1)/\varepsilon(\upsilon_2)$ = constant), then it follows that

$$R(\upsilon_1) = a_0 + a_1\, R\,(\upsilon_2) \qquad (3)$$

where a_0 and a_1 are constants. The constants a_0 and a_1 can thus be determined from two or more sets of observations, $R(\nu_1)$ and $R(\nu_2)$, corresponding to two or more fractional cloud cover conditions. Given a_0 and a_1, one can find the intersection of this linear relationship with the curve defining the "opaque" cloud condition which is obtained by radiative transfer calculation (i.e., simulation) using a prescribed temperature and moisture channel and assuming the opaque cloud condition at each pressure level. Figure 5 shows an example of this method applied to the same data used in the "slicing" demonstration of figure 4. In this plot each solid box corresponds to a different opaque cloud pressure level. (The cloud height order corresponding to lowest to highest radiance is 200, 250, 300, 350, 400, 500, 700 and 850 mbs., respectively.) It can be seen that with this method, the water vapor and CO_2 channels yield almost the same cloud pressure height estimate, alleviating the deficiency discussed earlier related to the spectrally independent emissivity assumption of the "slicing" method. However, it should be remembered that the "simulated" opaque cloud condition radiances depend on the absorbing gas profile which is much less certain for highly variable water vapor than it is for uniformly mixed carbon dioxide.

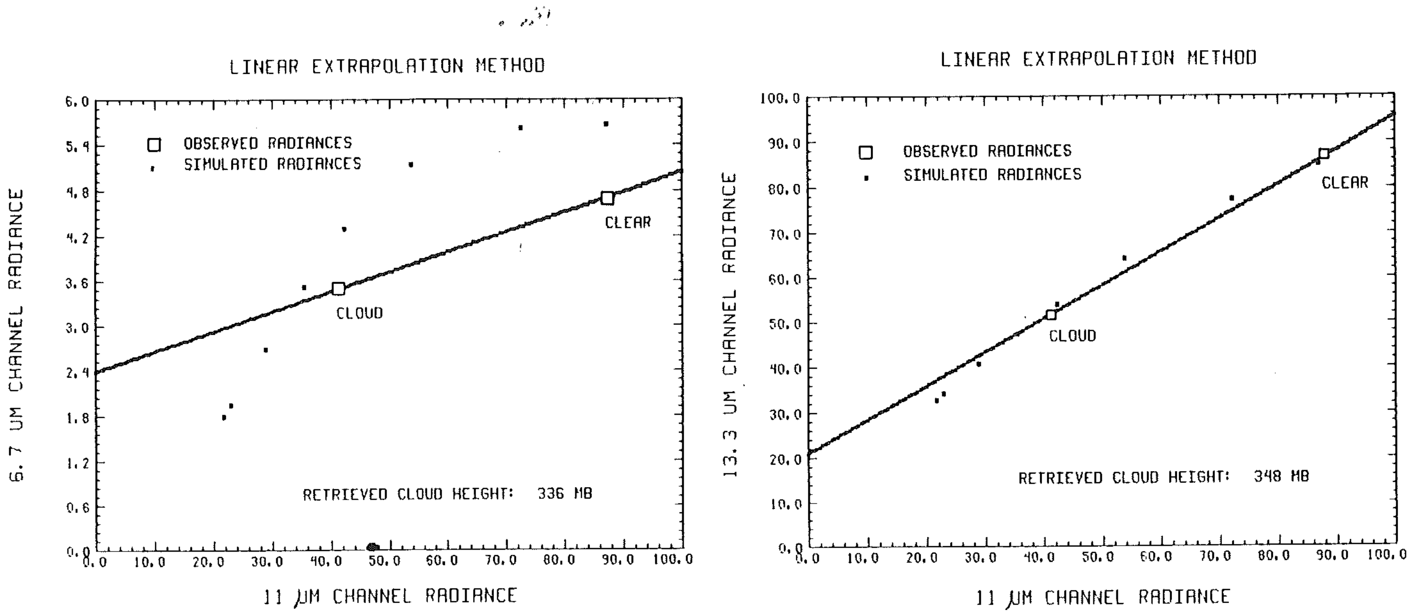

Figure 5: Illustration of the "Linear Extrapolation" method. The straight line represents the linear relation between the radiances observed in two spectral channels which results from a variation in "effective" cloud amount. The curve formed by the squares on each diagram shows the non-linear relation between the observed radiances which would result from the altitude variation of an opaque cloud filling the instruments field of view (i.e., effective cloud amount=1.0).

4. Example Cloud Estimates

Cloud heights were calculated using 6.7 μm water vapor, 11 μm window, and 13.3 μm CO_2 channel radiances for the bandwidths shown in figure 1. Variations in the bandwidths corresponding to variations between the spectral responses of the different satellite instruments

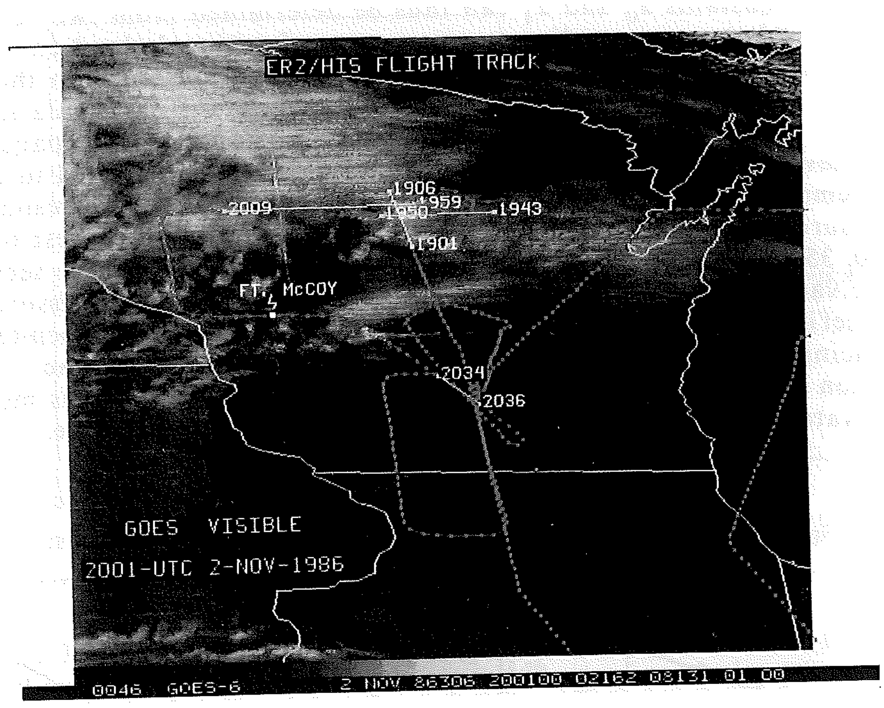

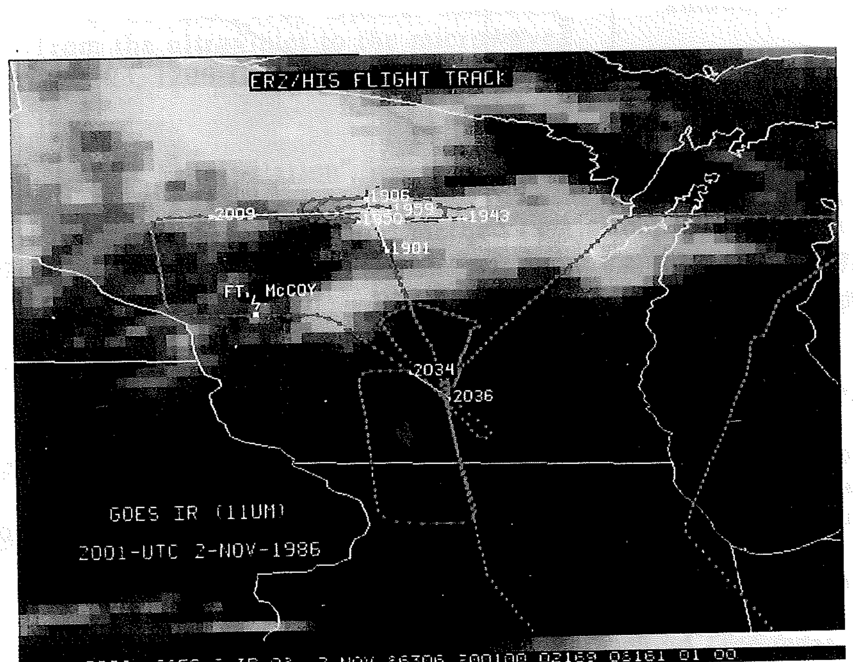

did not produce a significant variation in the results to be shown. As mentioned earlier, the case study day is 2 November, 1986. Figure 6 shows the flight track of the NASA ER-2 aircraft over GOES visible and 11 μm window imagery near the time of the cloud height determinations from the ER-2 HIS data. Extensive "cirrus" cloud is seen over central Wisconsin beneath the flight track of the ER-2. The position of the "Ft. McCoy" radiosonde observation at 2000 UTC is also shown since it was used for all the radiative transfer calculations needed for the application of each method.

Figure 7 shows for a small portion of the ER-2 flight track the variation of observed brightness temperature for each of the three spectral channels superimposed upon a vertical cross-section of LIDAR range normalized backscatter. In this and subsequent images, the white regions correspond to significant backscatter produced by cloud particles. Although these images reveal that a distinct top to Cirrus cloud is sometimes difficult to

Figure 6: Flight tracks of the ER-2 over Wisconsin on November 2, 1986. (a) Visible image and (b) 11 μm window image from the GOES-VAS.

distinguish, a high density of intense backscatterers at cloud top is normally present.

Figure 7b shows the pressure altitude estimated from 6.7 μm and 11 μm brightness temperature observations using the brightness temperature versus opaque cloud altitude curves shown in figure 2. It can be seen that both spectral regions tend to overestimate the cloud pressure (i.e., underestimate the cloud height). In the left hand portion of the plot where the cloud appears to be most dense, both the 11 μm and the 6.7 μm brightness temperatures provide a reasonable indication of the cloud height. In other portions of the plot the 11 μm brightness temperature estimate is much too low in altitude, apparently because of the transmission of warm surface radiation through the cloud. The water vapor channel brightness temperature produces a much more accurate estimate, even where the cloud is transparent, because the clear sky water vapor radiation is only slightly higher than

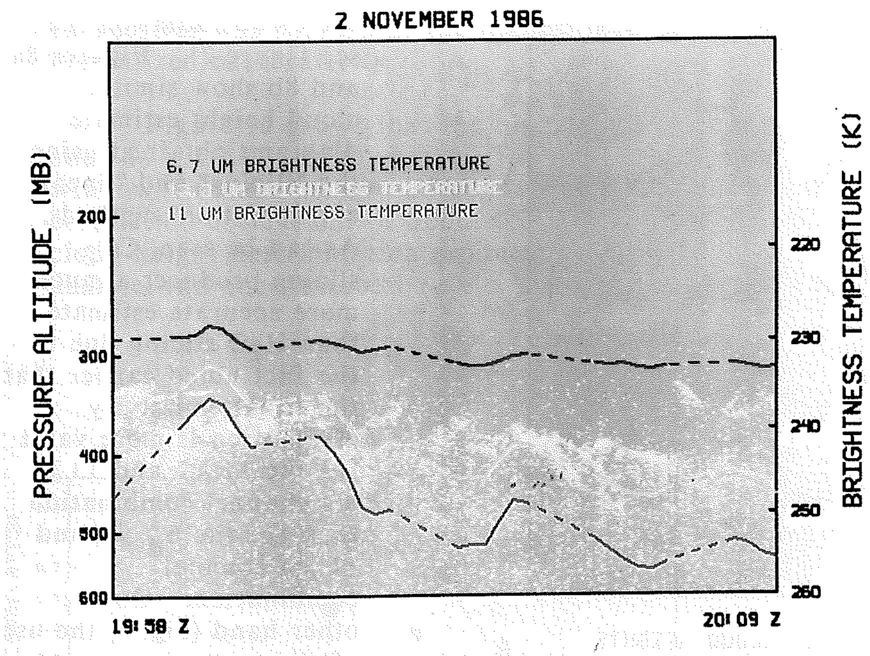

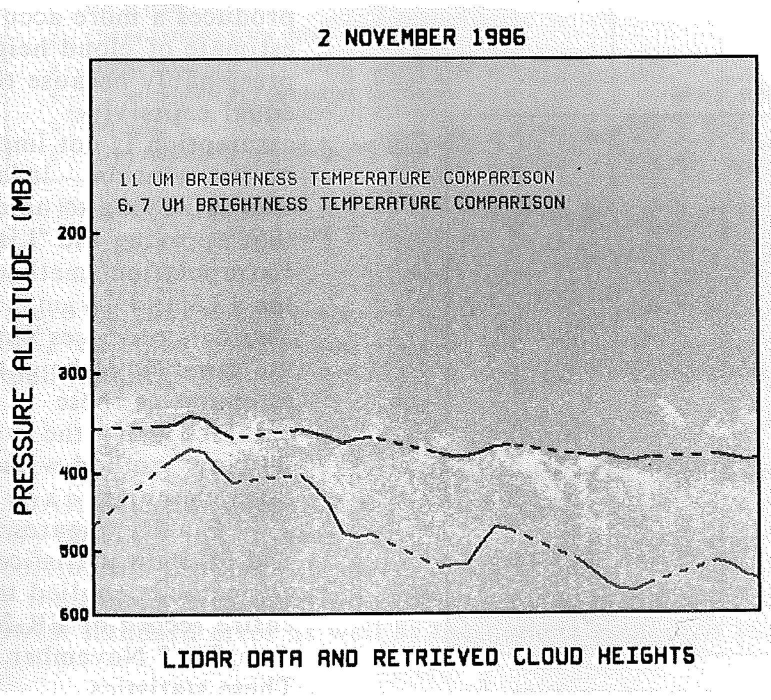

Figure 7: (a) 6.7 μm, 13.3 μm, and 11 μm brightness temperature observations superimposed over LIDAR backscatter cross-section, (b) Cloud pressure altitudes determined by the "Brightness Temperature Comparison" method.

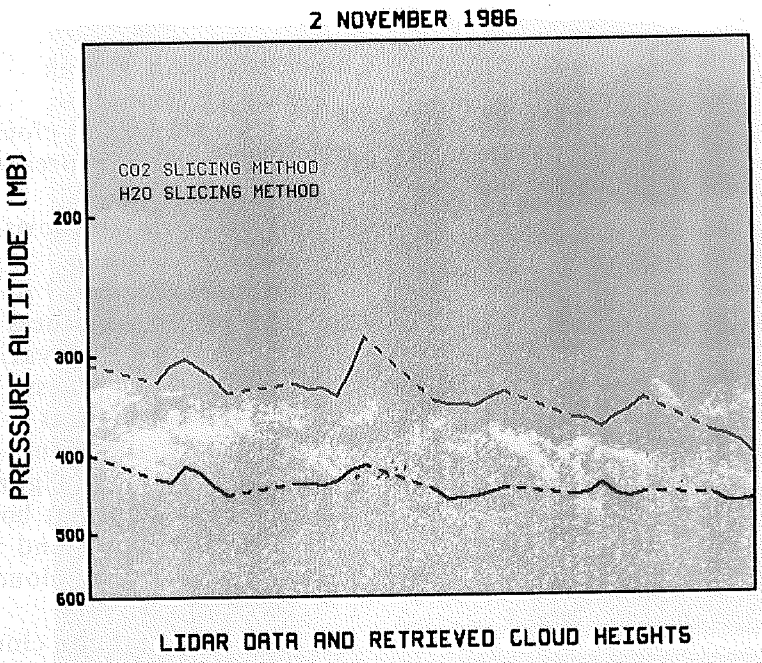

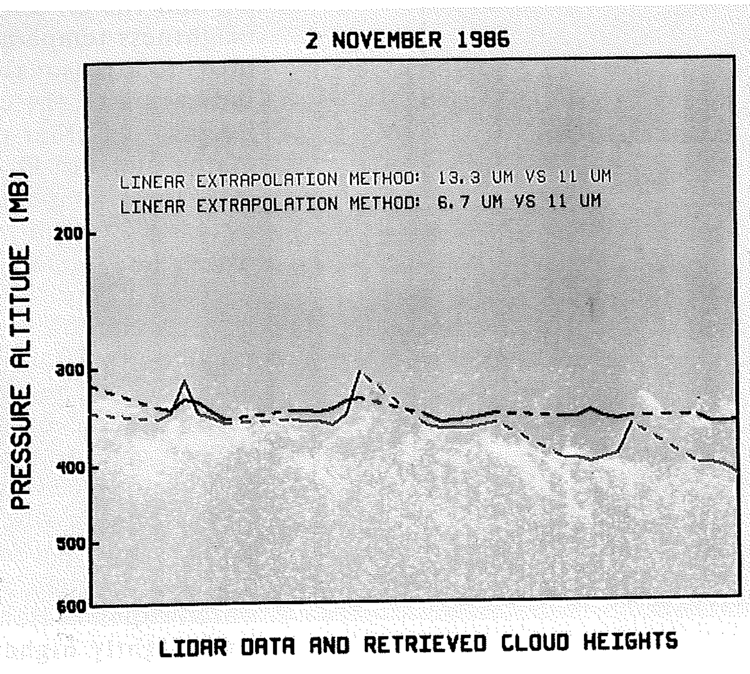

the cloud radiation (i.e., see figure 2). Figures 8a and 8b show similar cloud height estimate diagrams obtained using the "slicing" and "linear extrapolation" methods. As can be seen, CO_2 slicing produces a much more accurate estimate than H_2O slicing due to the fact noted earlier that the equal emissivity assumption is more valid for the 11 μm and 13.3 μm channel combination than for the 6.7 μm and 11 μm channel combination. On the other hand (fig. 3) the use of the water vapor channel with the linear extrapolation method produces a more accurate estimate of cloud height, presumably because the equal emissivity assumption is not imposed on the solution. It is also satisfying to note that applying the "Linear Extrapolation" method to the 13.3 and 11 μm channels produces almost the same cloud height estimates as those obtained using the "Slicing" method with the same channels.

Finally, figures 9a and 9b show statistics for all methods applied to the entire record of ER-2 data for 2 November. These statistics correspond to seventy-five independent intercomparisons of cloud

Figure 8: Cloud pressure altitudes determined by (a) "Slicing" and (b) "Linear Extrapolation," superimposed upon vertical cross-section of LIDAR backscatter.

height retrievals with coincident LIDAR observations. (The cloud height from the LIDAR backscatter was defined as the highest level where there was a sharp increase in the range normalized backscatter.)

Figure 9a shows that the highest correlation between the infrared determined cloud height and the LIDAR was close to 0.8 for the CO_2 "Slicing" method. The use of CO_2 radiance with window radiance using the "Linear Extrapolation" method possessed the next highest "skill" (i.e., correlation coefficient of about 0.7). The use of the 6.7 μm water vapor channel radiance for cloud height determination produced accuracies inferior to those achieved with a carbon dioxide channel radiance, the best results being achieved using the "Linear Extrapolation" procedure.

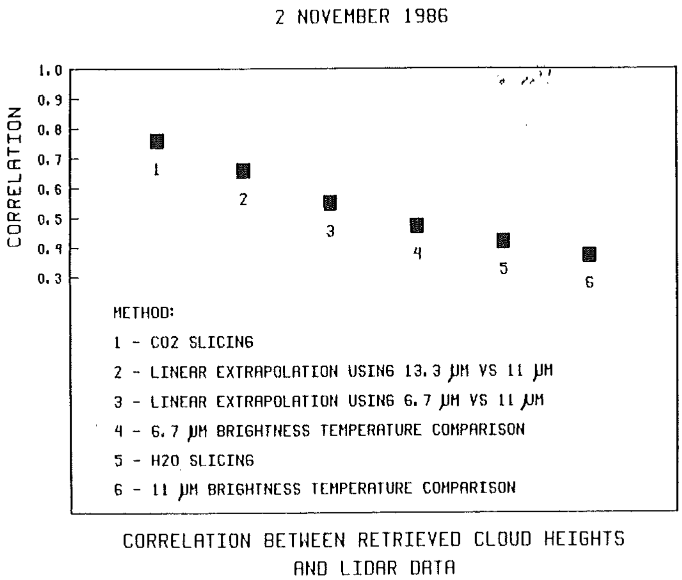

Figure 9a: Linear correlation between retrieved cloud heights and LIDAR observed cloud height.

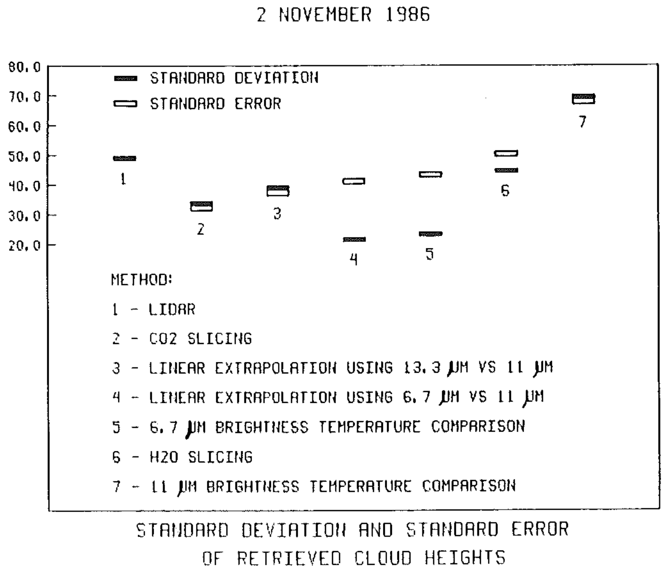

Figure 9b: Standard deviation and standard error (relative to LIDAR) of the retrieved cloud heights.

Finally, figure 9b shows the standard deviation and the standard error, relative to the LIDAR determinations, of the various infrared channel estimates. Here we see that only the CO_2 "Slicing" and "Linear Extrapolation" methods using the CO_2 and window channel combination produces standard errors less than the variability (i.e., standard deviation). The use of the carbon dioxide/window channel combination for cloud height estimation produces the lowest standard error as well as the highest explained variance of all the methods studied here.

5. Conclusions

In this study, methods currently used for estimating cloud height from Japanese, United States, and European satellites were tested using airborne interferometer spectral radiance observations and LIDAR measurements of cloud altitude. The most accurate results were those obtained using a combination of 13.3 μm CO_2 and 11.1 μm "Window" channel radiances. The use of 6.7 μm H_2O channels radiances produces a significant improvement over results achieved with 11.1 μm window radiances alone; however, the water vapor channel results are still significantly inferior to the CO_2 channel estimates. The inclusion of a 13.3 μm CO_2 channel on future geostationary satellite imaging radiometers should improve the utility of cloud tracked winds for meteorological applications.

References

Menzel, W.P., W.L. Smith, and T.R. Stewart, (1983) "Improved cloud motion wind vector and altitude assignment using VAS." J. Appl. Meteor., **22**, 377-384.

Revercomb, H.E. et al., (1988) "Radiometric calibration of IR Interferometers: Experience from the High-Resolution Interferometer Sounder (HIS) aircraft instrument." Advances in Remote Sensing Retrieval Methods, A. Deepak, H.E. Fleming, and J.S. Theon, Eds. (Deepak Publishing, Hampton, VA), 89-101.

Schmetz, J. et. al., (1989) "Operational evaluation of METEOSAT data." Annalen der Meteorologie, **23**, 210-211.

Smith, W.L., and R. Frey, (1990) "On cloud altitude determinations from high resolution interferometer sounder (HIS) observations." J. Appl. Meteor., **29**, 658-662.

Smith, W.L., and C.M.R. Platt, (1978) "Comparison of satellite-deduced cloud heights with indications from radiosonde and ground-based laser measurements." J. Appl. Meteor., **17**, 1796-1802.

Spinhirne, J.D., M.Z. Hansen and L.O. Caudill, (1982) "Cloud top remote sensing by airborne lidar." Appl. Optics, **21**, 1564-1571.

Szejwach, G., (1982) "Determination of semi-transparent cirrus cloud temperature from infrared radiances. Application to METEOSAT." J. Appl. Meteor., **21**, 384-393.